Optimal energy management of a photovoltaic-batteries-grid system

Diana Sabah Obaid[1], Ali Jafer Mahdi[2], Mohammed Husham Alkhafaji[1]
[1]Department of Electrical Engineering, University of Technology, Baghdad, Iraq
[2]Department of Electrical and Electronic Engineering, University of Kerbala, Karbala, Iraq

Article Info

ABSTRACT

Microgrid becomes an attractive concept to meet the rapidly increasing demands for energy in worldwide and deal with air pollutions. Distributed energy resources (DERs) in microgrid are the vital role to meet the demand of the grid locally. The performance and the photovoltaic (PV) source grid connected system's response depend on vital parameters like transient response, voltage or current overshoot, steady state error, and harmonics distortions. This research aims to optimize the proportional-integral (PI) controller for improving power quality performance and energy management of the PV battery of three phase inverter of grid connected mode scheme. Besides to the PI conventional method, three different meta-heuristic optimization algorithms are proposed and implemented in order to enhance the PI and hence all system parameters. These three algorithms are particle swarm optimization (PSO), whale optimization algorithm (WOA), dragonfly algorithm (DA) that can tune the PI controller's parameters by minimizing voltage regulator error, hence approving the goal of optimization in finding the optimal local or global solutions. The experimental results have been demonstrating the variety and the effectiveness of these optimization methods in convergence generation, computation time, and improving all required system parameters.

Corresponding Author:

Diana Sabah Obaid
Department of Electrical Engineering, University of Technology
Industrial Road, Bagdad, Iraq
Email: eee.19.38@grad.uotechnology.edu.iq

1. INTRODUCTION

A typical photovoltaic (PV) system of three phase inverter in grid-connected mode system has two sides (the PV and utility grid sides), as well as an important regulating stage. From a PV system, it contains the maximum power point tracking (MPPT) utilizing the perturbation and observation (P&O) algorithm, boost converter, storage, Bi-directional converter, inverter, LC-filter, transformer, and variable AC loads, as shown in Figure 1. The output terminal of the boost connected to the DC link capacitors where its output develops the input voltage of the inverter system. The available extreme power from the PV generator reached by using the boost converter with MPPT algorithm. The battery coupled to the DC-buss voltage through DC/ DC bi-directional converter is utilized to control charging and discharging of ESS.

The PI controller is a conditional-based load control feedback loop constructed using a linearized system equation [1]. The major standards for choosing this controller for managing an inverter are good performance of control, ease of implementation, and high reliability. The PI controller is used by the majority of AC system regulators of voltage and current to control grid current and voltage of the DC link, allowing inject the active power into the grid to be appropriately controlled and the inverter system's DC link voltage

to be stabilized. This is because the nonlinearity behavior of the inverter and loads has a significant impact on the system's harmonics, both voltage and current, resulting in the overall power system's failure [2]. Many studies in the stability of the controlling field were focused on the PI controller design for inverters connected to grid with the use of an inductive capacitance filter. Furthermore, the inverter stability problem with LC filters grid-connected is annualized in [3]. Although PI controllers are generally easy to tune, provide acceptable variations in the load conditions and grid disturbances [4], conversely, this control attitude involves the evaluation of all variables that affect the condition of the system, which brings about more complication and time consumption for the inverter system to reach to the optimal with fully resilient system.

To resolve this issue, extensive researches that combine PI controller with optimization methods have been done. These simulation results establish that the PI controller combined with optimization approaches produces excellent results in terms of total harmonic distortion (THD) in various optimization techniques [5]. Among those optimization approaches, fuzzy logic controllers (FLC), genetic algorithms (GA), artificial neural networks (ANN), and machine learning (ML) have good efficiency of tracking the global maxima, but their ability to track optimum solution is dependent on substantial model training, which requires a powerful approach and large amount of processing time. Therefore, the needing to the optimization algorithms that has a simple set of parameters with less time for converge to an optimal solution.

Also, the optimization algorithm does not involve corollaries rules while in operation linked to fuzzy logic controller also the neural fuzzy logic, it needs a time-consuming trial and error procedure. On the other hand, meta-heuristic techniques for example particle swarm optimization (PSO), whale algorithm optimization (WAO), cuckoo search optimization (CSO), grey wolf optimization (GWO), dragonfly algorithm optimization (DAO), artificial bee colony (ABC), and ant colony optimization (ACO). Can improve the efficiency by exploiting random numbers, offering feasible solutions, and sharing the information.

The aim of this study is to optimize the proportional-integral (PI) controller for improving power quality performance and energy management of the PV battery of three phase inverter of grid connected mode scheme by finding the best values of PI controlling to minimize transient response, eliminate overshoot, and achieve minimal steady-state error related to demand variation. By reducing the error between the regulators of controllers of voltage and current, frequency deviation, and THD of three phase PV systems, optimization techniques are used to properly design the PI controller settings.

The contribution is using different three optimization techniques and compare among them which give the best parameters of PI controller of the system. Apply this system to achieving extra economical operation of the electric grid, improving reliability with different energy resources and the possibility to change the load profile by companies. The limits of load power of the system are (100-250) kW, voltage $(400) \pm 10\%$ V, and the frequency (50) $\pm 2.5\%$ Hz.
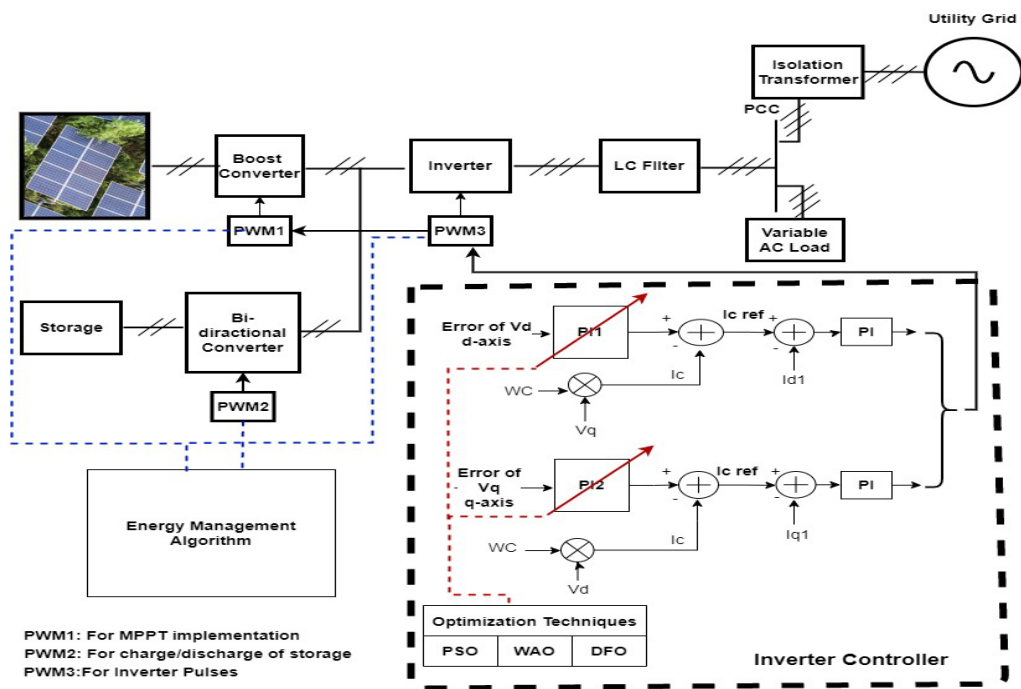

Figure 1. Proposed controlled system with optimization techniques

2.   PV INVERTER HYBRID GRID-CONNECTED SYSTEM

The hybrid system composed of the PV generator plant that coupling to DC bus through DC/DC unidirectional boost converter; because of there is no DC load connected to DC bus, a unidirectional three phase inverter DC/AC is used to supply the grid by AC power with same voltage and frequency. Battery storage is used in energy storage system to store and dissipate the energy via DC/DC bidirectional converter. An LC filter used on the output terminals of the inverter to refine and produce pure sinusoidal waveforms for voltage and current, all the component will be discussed in next sections, Figure 1 show the block diagram of hybrid system.

3.   MODELING OF THE SYSTEM

3.1. PV generator design

PV arrays the main elements are the photovoltaic cells. When exposed to the sun's rays, it converts solar energy into electricity [6]. PV contains short circuit current (I_{sc}), open-circuit voltage (V_{oc}), voltage of max. power point (V_{MPP}) and current of max. power point (I_{MPP}). These parameters form the curves of I-V and P-V. The model of single and two diodes are employed to simulate a PV. The two diodes are the major standard model However; further variables are necessary to create the model more multifaceted [6]. The basic single diode PV module current is signified by [7].

A PV array consisting of any number of PV modules that are wired in series and/or parallel to deliver particular voltage and amperage as require. The total generated power that is proposed in this work is (200 kW). The selected type of the array is "SunPower SPR-415E-WTH-D".

The maximum power of "SunPower SPR-415E-WTH-D"=400.221 W for each array, for (200 kW) the total of number of the arrays is given by [8]:

$$N = \frac{Total\ generated\ power\ (watt)}{Maximum\ power\ for\ each\ array\ (watt)}$$

$$N = \frac{200\ kW}{400.221\ W} = 499.72\ array, we\ will\ chose\ 504\ array\ panel. \tag{1}$$

The PV array farms consist of parallel and series arrays interconnected and arranged in specific manner to produce a specific voltage and current as required in design process, the N_p and N_s represent the number of the parallel and series arrays respectively and they can be given in the following expression:

$$N = Np * Ns \tag{2}$$

the total number of arrays in series N_s can be calculated from [9]:

$$N_s = \frac{Vdc\ input\ to\ the\ Boost}{V_{mpp}\ for\ array} \tag{3}$$

where,

$$V_{L-L\ (rms)} = 0.6124 * m * Vdc \tag{4}$$

where m is the modulation index and is chosen as 0.8 and the $V_{L-L\ (rms)}$ is 400V, and then the Vdc of inverter is equal to 816 V, choose Vdc of the inverter 800 V. In case of boosting the PV voltage, the duty cycle of the boost converter is taken 0.18 to reach the required DC-link voltage. The output voltage of PV is the input voltage of Boost converter=656.1

$$N_s = \frac{656.1}{72.9} = 9$$

The total number of arrays in series N_s is 9, by applying (2), the total number of arrays in parallel N_p is [9]:

$$N_p = \frac{504}{9} = 56\ array$$

3.2. DC/DC boost converter

The unidirectional boost converter in this work is used to improvement the DC voltage from 656 V to 800 V. This converter yields a MPPT technique to extract the max. power generated from PV by varying the duty cycle (D). Figure 2 shows the circuit equivalent of unidirectional boost converter [10], [11].

3.3. BESS

The charging and discharging of the battery characteristics method for long or short periods are defined in [12], [13]. There have been a variety of models for designing batteries battery storage system (BESS), but several type these batteries dose not used in electrical design because it has long time constant. Figure 3 explains how to use model of the resistive voltage source to make electrochemical evaluating easier.
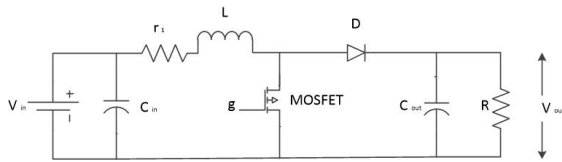
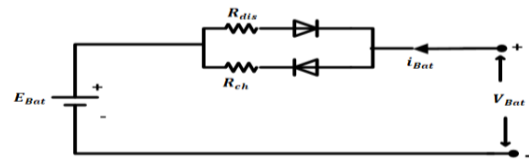Figure 2. Boost converter circuit   Figure 3. BSS equivalent circuit

where, E_{Bat} is the battery's electromotive force (E.M.F), R_{ch} is the internal charging resistance and R_{dis} is the discharging resistance, Both of these factors add to energy loss within the storage battery in either states of its operation, i_{Bat} is the current of charging also discharging, the charging current have positive value of i_{Bat} and the discharging current have a negative value of i_{Bat}, and V_{Bat} characterizes the terminal voltage of the battery. In this model, E_{Bat} and electric parameters R_{ch} and R_{dis}, all reliant on battery state of charge (SOC), and (T_{emp}) is the battery operating temperature shown in (5) [14]:

$$V_{Bat}(SOC, T_{emp}) = E_{Bat}(SOC, T_{emp}) + i_{Bat} R(SOC, T_{emp}) \tag{5}$$

3.4. Bi-directional DC/DC converter design

The polarity of the input voltage is known to change when the direction of power flow in a current source inverter is changed. In the meantime, the DC current flow is always in the same direction. Because the proposed inverter is powered by a battery, a change in polarity of the battery terminal voltage is unacceptably disruptive to the battery system's regular operation. As a result, a DC/DC converter is required to manage bidirectional power flow while maintaining the necessary polarity at the battery terminals and the required DC current direction at the inverter side [15].

Figure 4 show the the bi-directional DC/DC converter, the structure is shown in Figure 4(a), which controls either charging or discharging of the battery. Boosting scheme is used in the construction of bi-directional DC/DC converters; the implication is that the DC-link voltage is continuously higher than the battery voltage. To accomplish two-way power alteration [16]. Both S_1, and S_2 of the DC/DC converter control system switches are regulated. The battery current is regulated by the inner current loop in order to monitor the provided command i_{Bat}^* Figure 4(b). The DC-link voltage is controlled by the outer voltage loop, which serves as a reference signal for the inner loop i_{Bat}^* [17], [18].
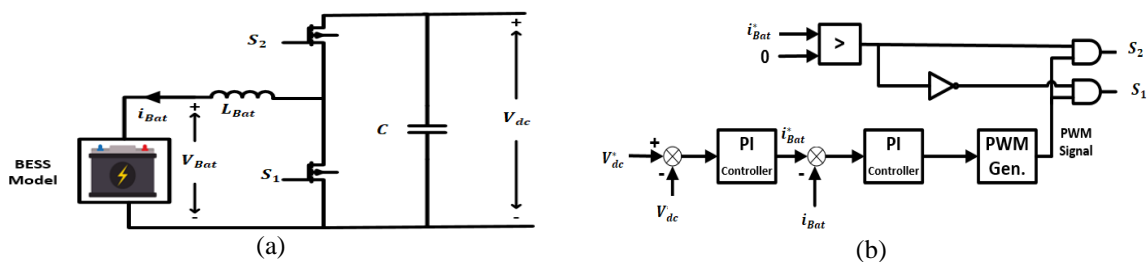
Figure 4. Control system of BESS where: (a) structure and (b) blok diagram

3.5. The angle beta (β) and voltage ripple

At steady state, the voltage of the DC-link $v_{dc}(t)$ can be expressed as following:

$$v_{dc}(t) = v_a + \sum_{n=1}^{\infty} b_n \cos(n\beta t + \emptyset_n) \tag{6}$$

where v_{dc} is the mean value of the DC_link voltage b_n and $\emptyset_n$ magnitude and phase for harmonics ($n^{th} -$ $order$) and β is the DC-link ripple frequency ($\frac{1}{t_{ripple}}$) (in radian) [19].

3.6. Droop control in grid side

Droop control is a controller system that simulates the synchronous generator (SG) output in order to control the inverter in the distributed system, as shown in Figure 5, [18]. The reactive power's overall size is shown by voltage droop characteristic curves. (Q-V) is utilized to regulate the voltage of the system, then by active power with frequency (P-f). During the control process, the droop controller will provide a reference value for voltage also the frequency. In a system of distributed generator (DG), P-f and Q-V droop controls are usually used to control active and reactive power [10], [20], [21]. For a power generator to be stable, the control of frequency necessity has a drooping characteristic with regard to the output of generator, seen in Figure 5(a).

The characteristic of the power droop can be expressed in the equations [22], [23]:

$$f_r = f_n + k_p \ (P_n - P_r) \tag{7}$$

where f_r is reference frequency of grid, f_n is nominal frequency, P_r and P_n are a reference and nominal active power respectively, k_p is the coefficient of P-f droop. The power generators terminal voltage is proportional to the reactive power of the generator output and has a drooping characteristic. Shown in Figure 5(b). The characteristic Q-V droop is defined by the equation [21]:

$$V_r = V_n + k_v \ (Q_n - \ Q_r), \tag{8}$$

where k_V is reactive droop coefficients, V_r is the amplitude of the output voltage.
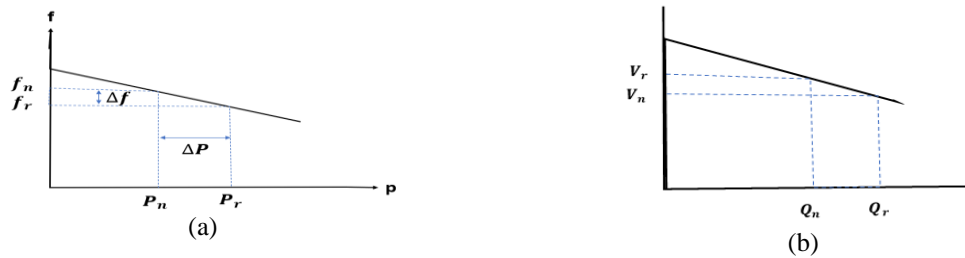

Figure 5. Characteristics of droop control: (a) P-f droop control and (b) Q-V droop control

4. OPTIMIZATION TECHNIQUES

The fitness function is the best answer for estimating the search area, also known as the objective function. The absolute error and the THD are expressed as objective functions to be minimized for the DC link voltage and current controller, for obtaining the optimal PI controller parameters Kp and Ki of either D or Q in the regulator of the DC link voltage [3]. The system's objective function can be summarized as follows:

$$Min \ F(x) = C1 \int_0^{T_{max}} t|e(t)|_{Vd}.dt + C2 \int_0^{T_{max}} t|e(t)|_{Vq}.dt + C3 \int_0^{T_{max}}$$
$$t|e(t)|_F.dt + C4 \int_0^{T_{max}} THD_V.dt \tag{9}$$

where e is the error, C1, C2, C3 and C4 are weight coefficients, T_{max} is the max. time, and THD_V is the total harmonic distortion of the output voltage.

4.1. PSO technique

The evolutionary algorithm of PSO technique was created by Elberhat and Kennedy to handle a number of real-valued optimization issues in 1995 [1], [4]. PSO is an effective strategy for finding the optimal clarification in a nonlinear system. The PSO algorithm is based on the natural behavior of flocks of birds and schools of fish moving around in groups in a D-dimensional world [4]. In each iteration, each particle in the

swarm advances in the direction of the best solution found so far in this. During the contact, the particle seeks for and advances toward a better solution than the previous one, thereby discovering the region carefully [23], [24]. The position and velocity of the i-th particle of the swarm in the search space vector are represented as $X_i=[X_{i1}, X_{i2},...,X_{iD},]$ and $V_i=[V_{i1}, V_{i2},...,V_{iD},]]$, respectively [25]. The best previous solution for the i-th particle swarm is $P_i=[P_{i1}, P_{i2},...,P_{iD},]$ and the global best position is $P_g=[P_{g1}, P_{g2},...,P_{gD},]$ [26], [27].

In the next iteration, each particle's position and velocity will be modified based on (10) and (11) [28], [29], respectively, as shown in Figure 6.

$$V^{n+1}{}_i= \text{w}V^n{}_i + C_1 r_1(P^n{}_i - X^n{}_i) + C_2 r_2\left(P^n{}_g - X^n{}_i\right) \tag{10}$$

$$X^{n+1}{}_i=X^n{}_i+V^{n+1}{}_i \tag{11}$$

Where (i = 1, 2, ..., m), m is the of number iteration, ω is the weight of inertia, C1 is the social rate, C2 is the cognitive rate, and r1 and r2 are random intervals (0, 1).
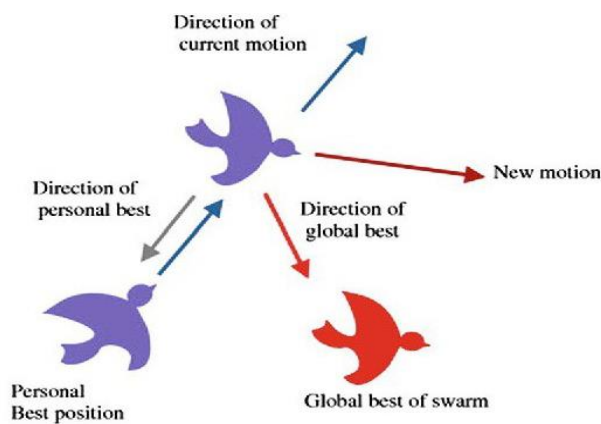

Figure 6. Particle trajectory analysis in PSO

4.2. DAO technique

Dragonfly algorithm optimization proposed by Mirjalili in 2015. Dragonflies (Odonata) are beautiful insects. This insect has almost 3,000 different species all over the world [30]. A dragonfly's lifecycle includes two Neural Compute and the main indicators: nymph and adult. They expend the main portion of their lifetime in nymph, and they undergo metamorphism to become adult [30]. Nymph dragonflies also precede on other marine insects and even small fishes. The peculiar and frequent swarming behavior of dragonflies is a remarkable fact. As shown in Figure 7, the Dragonflies swarm only for two reasons: migration as shown in Figure 7(a), or hunting as shown in Figure 7(b) The first is known as a dynamic (migratory), whereas the second is known as a static (feeding) swarm. Dragonflies form tiny collections and fly back and forth over a small area to hunt smaller flying preys like butterflies and mosquitoes in a static swarm [31]. Local movements and sudden shifts in the flying path are the main features of a static swarm. Swarms of dragonflies that fly in a single direction across long distances constitute dynamic swarms [32]. The source of these swarming behaviors is the core inspiration of the DA algorithm, both static and dynamic. The two key points of optimization utilizing meta-heuristics are exploration and exploitation, which are extremely comparable to these two swarming behaviors The major goal of the exploration phase is for dragonflies to form sub-swarms and fly over different places in a static swarm. Dragonflies in the static swarm, on the other hand, fly in larger swarms and in one direction, which is advantageous in the exploitation phase [33]. The following equations mathematically represent these two phases, as follows:
a)   Select a food source from archive: X^+=SelectFood(archive).
b)   Select an enemy from archive: X^-=SelectEnemy(archive).

$$\text{Update step vectors using } T(\Delta x) =\left|\frac{\Delta x}{\sqrt{\Delta x^2+1}}\right| \tag{12}$$

$$\text{Update position vectors using } X_{t+1}=\{-X_t \ r < T(X_{t+r}) \ -X_t \ r \geq T(X_{t+r}) \tag{13}$$

(a)   (b)
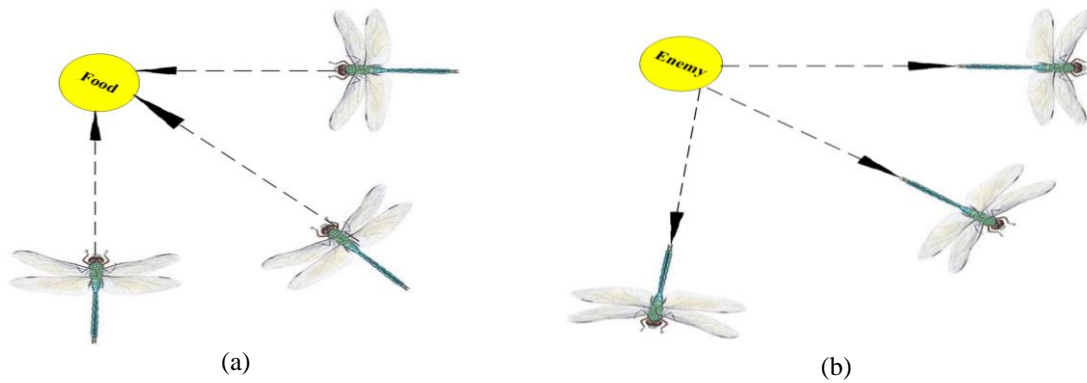
Figure 7. Behavior of dragonflies where: (a) attraction of food and (b) distraction from enemy

4.3. WAO technique

Whale algorithm is proposed for optimizing numerical problems by Mirjalili and Lewis, in 2016. Whales are magnificent animals. They are regarded as the world's largest mammals. An adult whale can reach a length of 30 meters and a weight of 180 tons. Killer whales, Minke whales, Sei whales, humpback whales, right whales, finback whales, and blue whales are among the seven primary species of this enormous mammal. Whales are primarily thought of as predators. Because they must breathe from the ocean's surface, they never sleep. Half of the brain, in truth, only sleeps. Whales are amazing animals because they are thought to be very intelligent and emotional. According to Hof and Gucht [34], whales have common cells in certain areas of their brains similar to those of human called spindle cells. Humpback whales' unusual hunting style is the most fascinating feature of their biology. This sort of searching is referred to as the bubble-net feeding method [35]. Humpback whales tend to hunt krill or small fish near the surface of the water. Blowing regular bubbles along a circle or a '9'-shaped path has been noticed as a method of hunting. Prior to 2011, only surface observations were used to explore this tendency. However, Goldbogen *et al.* [36] studied this behavior utilizing tag sensors. They captured 300 tag-derived bubble-net feeding events of 9 individual humpback whales. They discovered two bubble-related moves that they dubbed 'upward-spirals' and 'double loops.' Humpback whales dive to a depth of around 12 meters, then begin to build a spiral of bubbles around their meal and swim up to the surface. Coral loop, lobtail, and capture loop are the three steps of the later maneuver shown in Figure 8. Goldbogen *et al.* [36] provides more details on these behaviors. It's worth noting that humpback whales are the only ones who practice bubble-net feeding. This work investigates the spiral bubble-net feeding maneuver mathematically in order to improve it. Update the position of the current search agent.

$$\vec{D} = |\vec{C} . \overrightarrow{X^*}(t) - \vec{X}(t) \tag{14}$$

Updating the position of the current search is achieved using the following formula:

$$\vec{X}(t + 1) = \vec{D}.e^{bl}, cos\ cos\ (2\pi l)\ + \overrightarrow{X^*}(t) \tag{15}$$
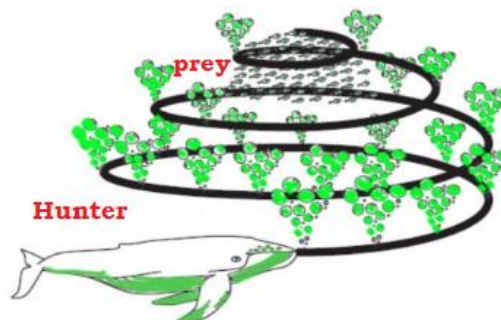

Figure 8. Humpback whale's behavior of bubble-net feeding [35]

5.   RESULTS AND DISCUSSION

MATLAB/Simulink with MATLAB-2018b version using to simulate the system of a 200 kW PV generation of power system whilst the implementation of the optimization algorithms is achieved through combining of the Simulink with m-file codes. The simulation parameters are listed in Table 1. During regular functioning the power generation system is connected to the grid. The PV is the main supplier of power demand in the system. Unless the PV system is unable to meet all of the loads, the power deficiency is covered by the storage system and the grid.

Table 1. Simulation parameters

Parameters	Values	Parameters	Values
Rated power	200 kW	Capacitor of Filter C_f	40 µF
Voltage of grid (L-L)	0.4 kV	Inductor of Filter L_f	0.815 mH
Frequency of Grid	50 Hz	Resistance of Bidirectional R	0.05 Ω
DC voltage	0.8 kV	Inductor Bidirectional L	0.3 mH
Switching frequency	10 kHz		

5.1. Effects of optimization techniques on PWM control signals

The application of optimization to decrease DC-Link ripple in a typical two-stage inverter drive circuit consisting of a boost converter cascaded by a three-phase full bridge inverter and a motor. The ripple time of the first harmonic of duty cycle was modified by the optimization strategies. The less frequent ripple time have largest value of β and low harmonics, because $cos\ cos\ β$ inversely proportional with the β in (6). It can be noted that from the Tables 2 and 3, Figures 9 and 10 the response of PSO faster than DAO, and WAO, the response of DAO is faster than the response of WAO so the best optimization technique is WAO.

Table 2. Boost converter duty cycle performance (D1) with irradiance of 1000 W/m², 25 °C and load change (150-250) kW

Performance index	PSO	DAO	WAO
Ripple period (ms)	18.800	18.20	19.50
Ripple frequency (Hz)	54.900	53.19	51.28
β =2πf (rad)	344.94	334.2	322.2

Table 3. Bi-directional converter duty cycle performance (D2) with irradiance of 1000 W/m², 25 °C and load change (150-250) kW

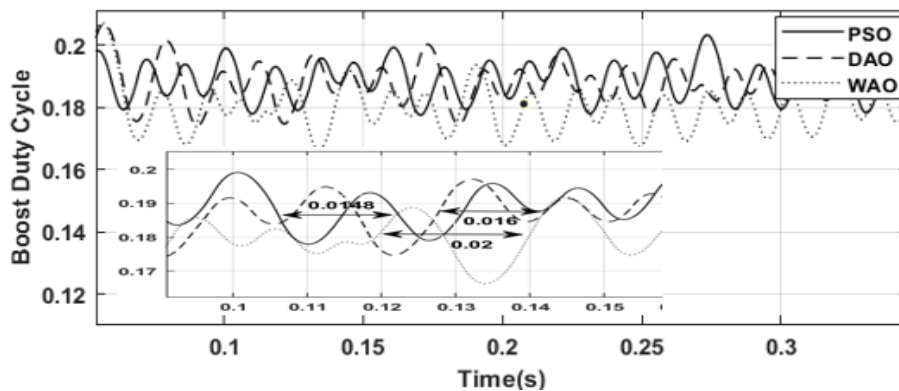| Performance index	PSO	DAO	WAO
Ripple period (ms)	14.800	16.00	20.000
Ripple frequency (Hz)	67.560	62.50	50.000
β =2πf (rad)	424.49	392.69	314.159

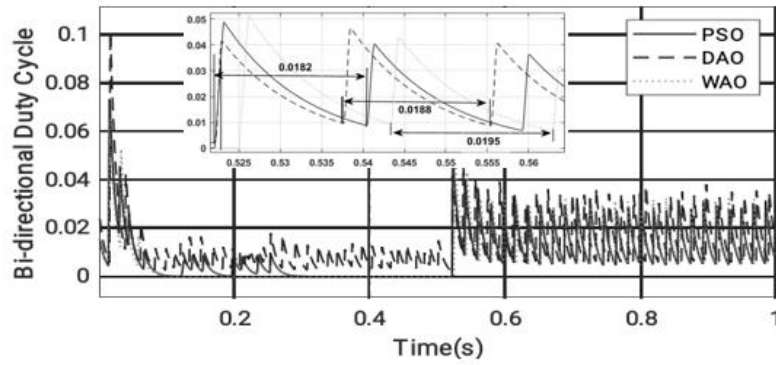Figure 9. Duty cycle of boost converter (D1)

Figure 10. Bidirectional duty cycle (D2)

5.2. Effects of optimization techniques on DC buss voltage

The system operates initially with load power of 150 kW. On time of 0.5 s, the demand on the grid system suddenly increased to 250 kW. Figure 11 clarify a comparison of the DC link voltages results of three algorithms of optimization technique of tuning PI controllers (PSO, DAO, and WAO) when the irradiation 500 W/m^2 and the temperature of 25 °C, and Figure 12 when the irradiation 1000 W/m2 and the temperature of 25°C. From the results, the rise time of the WAO is less than DAO also DAO is less than PSO, the values is shown in the Tables 4 and 5. Because the DC link voltage with WAO method responds quicker than the both DAO and PSO techniques in stabilizing the DC input voltage for the inverter system. Also, at time of 0.5 s. Moreover, the PI controller with the WAO method has return to the steady-state condition faster than the DAO controller, and DAO faster than PSO. As a results, the optimization technique can adjust the effect of transient on the system in order to supply stable DC input to the inverter depends on the type of technique as shown in Tables 4 and 5.
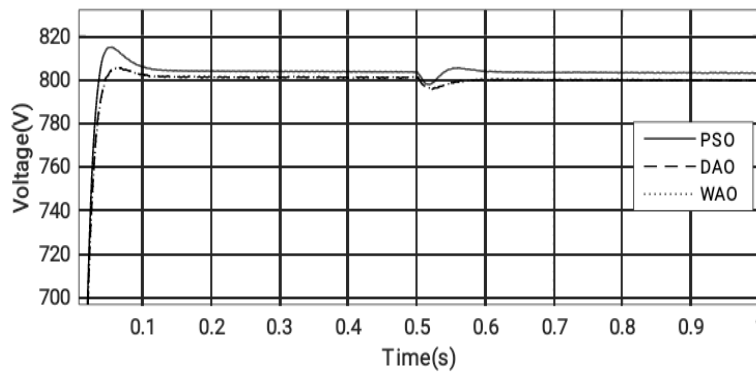

Figure 11. DC-buss voltage of irradiation 500 W/m^2 and load change (150-250) kW
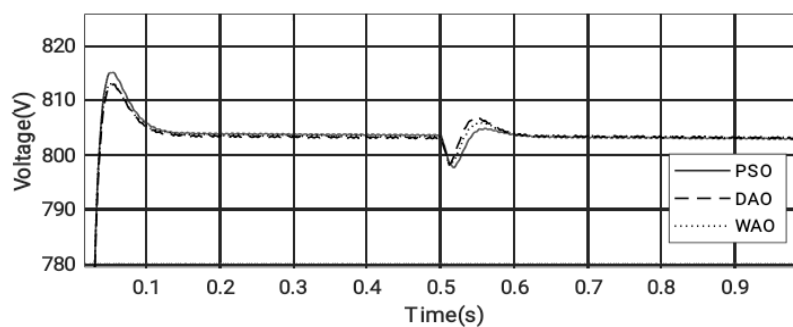

Figure 12. DC-buss voltage of irradiation 1,000 W/m^2 and load change (150-250) kW

Table 4. The performance of DC-link side at irradiance of 500 W/m^2 and load change (150-250) kW

Performance index	(0-0.5) sec.			(0.5-1)sec.		
Optimization technique	Voltage overshoot (V)	Voltage undershoots (V)	Settling time (ms)	Voltage overshoot (V)	Voltage undershoots (V)	Settling time (ms)
PSO	1.63	-	77.8	1.5	-5.8	100.6
DAO	0.424	-	62.46	-	-4.4	70.5
WAO	0.424	-	62.46	-	-4.4	70.5

Table 5. The performance of DC-link side with 1000 W/m2 irradiance and load change (150-250) kW

Performance index	(0-0.5) sec.			(0.5-1)sec.		
Optimization technique	Voltage overshoot (%)	Voltage undershoots (%)	Settling time (ms)	Voltage overshoot (%)	Voltage undershoots (%)	Settling time (ms)
PSO	1.4	-	93.94	1.4	-0.734	96.8
DAO	1.169	-	65.44	3.3	-0.659	96.8
WAO	1.169	-	65.44	2.3	-0.659	96.8

5.3. Effects of using optimization techniques on frequency

The comparison of the frequency of the system with inverter of tuning PI controllers (PSO, DAO, and WAO) shown in Figure 13 when the irradiation 500 W/m^2 and the temperature of 25°, and Figure 14 when the irradiation 1,000 W/m^{2,} and the temperature of 25°. When the system operates with load power greater than generated power the BBS and the grid contribute to supply the load demand then the PI controller of droop control controlling the frequency deviation. On a time of 0.5 sec the load was increased and has drawn more current from the energy storage also grid to supply the load. When the load increases rapidly, the frequency responses of the PI controller with optimization methods are constant and more stable, because of the controller optimization algorithms correct the overshoot during any modifications, and the response depend on the technique used to optimize the PI controller as seen in Tables 6 and 7, the best response is when using WAO and then when using DAO, and then the PSO technique.
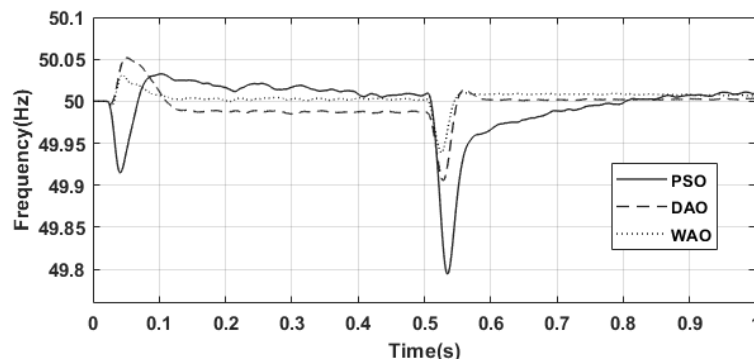

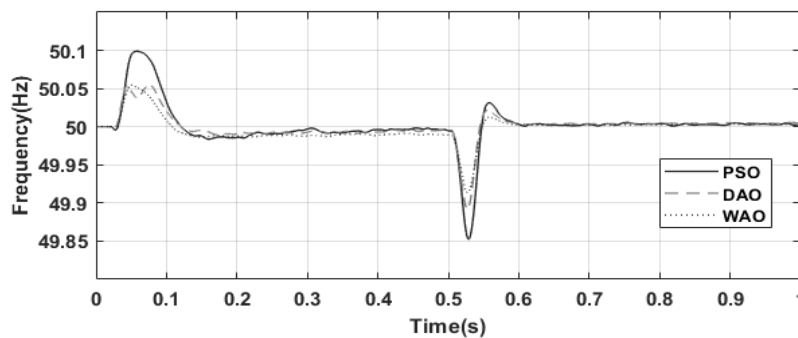Figure 13. Frequency signals of irradiation 500 W/m^2 and load change (150-250) kW

Figure 14. Frequency signals of irradiation 1,000 W/m^2 and load change (150-250) kW

Table 6. The performance of grid side with 500 W/m^2 irradiance and load change (150-250) kW

Performance index	(0-0.5) sec.		(0.5-1)sec.	
Optimization technique	Frequency deviation (%)	Settling time (ms)	Frequency deviation (%)	Settling time (ms)
PSO	-0.16	97.4	-0.42	198
DAO	0.10	80	-0.18	89.3
WAO	0.06	64.5	-0.12	54.9

Table 7. The performance of grid side with 1,000 W/m^2 irradiance and load change (150-250) kW

Performance index	(0-0.5) sec.		(0.5-1)sec.	
Optimization technique	Frequency deviation (%)	Settling time (ms)	Frequency deviation (%)	Settling time (ms)
PSO	0.2	125.2	-0.3	106.9
DAO	0.1	101.2	-0.22	87.1
WAO	0.1	85.8	-0.18	70

5.4. Effects of using optimization techniques on THD

In power system applications, the use of high-quality energy from a system of low harmonic content in consideration of current and voltage is critical, particularly when connecting to the three-phase grid. The cause for this is because a high-quality output power with a low THD factor on the voltage and current signal gives the user more constant and linear power, which saves energy. The grid system suffers from a high THD factor when it consumes less power factor. The THD factor of the output phase voltage and current can be decreased to an acceptable level of less than 5% by employing an upgraded controller and fast Fourier transform analysis, which satisfies the EEE Std. 929–2000 [37]. With the established optimization strategies, the voltage and current harmonic spectrum results display a percentage on the inverter output voltage and current shown in a Table 8. This illustrates a WAO reduce the harmonics more than the DAO and PSO, when the irradiation 500 W/m^2 and the temperature of 25° the harmonics of load current and voltage as shown in Figures 15-17. As a result, enhancing the inverter system's controller algorithm leads to improved system performance.

Table 8. THD of inverter voltage and current of 500 W/m^2 irradiance and Load change (150-250) kW

Performance index	PSO	DAO	WAO
Total voltage distortion (%)	1.86	1.84	1.65
Total current distortion (%)	4.73	4.61	3.87
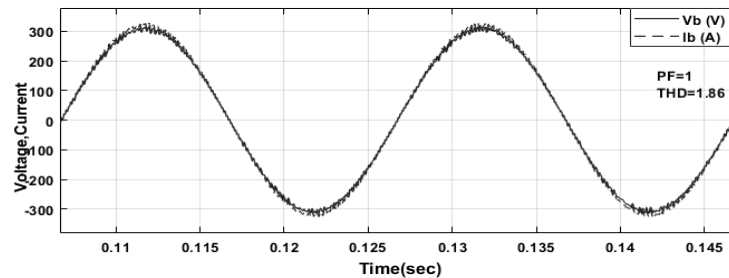
Figure 15. Load voltage and current of 500 W/m^2 irradiation and load change (150-250) kW using PSO algorithm
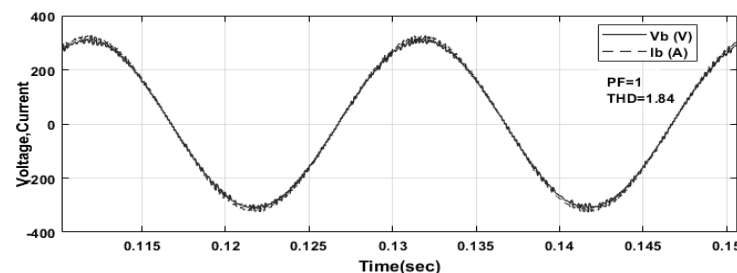
Figure 16. Load voltage and current of 500 W/m^2 irradiation and load change (150-250) kW using DAO algorithm
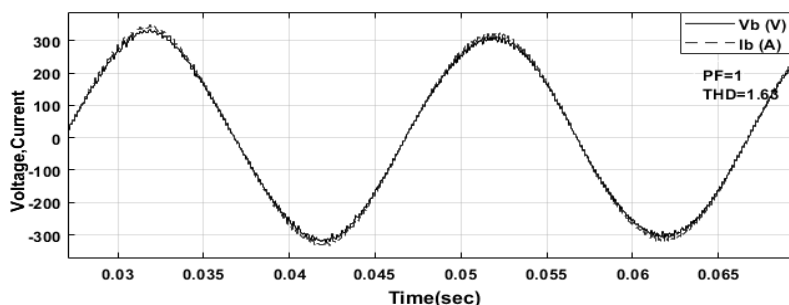
Figure 17. Load voltage and current of 500 W/m^2 irradiation and load change (150-250) kW using WAO algorithm

6.   CONCLUSION AND FUTURE WORK

The PI controller was widely often used, because of its flexibility and reliability, in synchronous reference frames, the optimization technique is used to discover the best settings parameters to PI controller through minimizing the error of regulator's voltage. The used of techniques is to identify the ideal PI controller parameters and decrease error as much as possible, and the percentages of THD for the voltage and current the inverter output and the load signals. You have to choose the right fitness function to find the goal using the technique. The comparison between optimization techniques shows which the best technique responses used to the control of the inverter to decrease voltage overshoot, response of transient, and steady-state error by determining the optimum PI controller parameters and lowering the error.

The study also discovered that when WAO is utilized, the THD percentages for the voltage and current of the inverter output signal are substantially less than when DAO and PSO are utilized, respectively, under varied loads. Additionally, the time it takes for the DC buss voltage to achieve the steady state condition is substantially shorter than for other techniques. Indicating rapid response under normal frequency of 50 Hz. In utilizing WAO technique, in terms of DC link fluctuation, voltage stabilization, harmonics decrease, and frequency constancy, it performs better. The use of optimization techniques in power system applications give a healthy controller can be employed for the inverter controller system, resulting in improved performance and improve the quality of power. We can use different techniques and chose the best of them and take which improve our purpose.

This is used to identify the best settings for the voltage regulator's PI controller parameters in a three-phase inverter system. According to the results, the DAO technique finds the best result faster than WAO and PSO, although WAO performs better in the controller than the DAO and PSO techniques in terms of finding the optimum values for the PI controller. For the future work, using artificial intelligence tools like nature inspired optimization algorithms. Integrating prediction algorithms for solar irradiance and load demand for load preparation and reduced a cost function related to energy pricing and gas releases can improve the energy management system. And the use of supercapacitor with the battery can be improving system stability.

REFERENCES

[1]   N. A. Selamat, T. O. Ramih, A. R. Abdullah, and M. S. Karis, "Performance of PID controller tuning based on particle swarm optimization and firefly algorithm," *International Journal of Recent Technology and Engineering (IJRTE)*, vol. 8, no. 3S2, pp. 225–230, 2019, doi: 10.35940/ijrte.c1042.1083s219.
[2]   Y. Ping, Z. Qunru, X. Zhirong, Y. Haozhe, and Z. Yuanhui, "Research on nonlinear phenomena of single-phase H-bridge inverter," in *2014 IEEE PES Asia-Pacific Power and Energy Engineering Conference (APPEEC)*, 2014, pp. 1-6, doi: 10.1109/APPEEC.2014.7066158.
[3]   S. Yang, Q. Lei, F. Z. Peng, and Z. Qian, "A robust control scheme for grid-connected voltage-source inverters," *IEEE Transactions on Industrial Electronics*, vol. 58, no. 1, pp. 202-212, Jan. 2011, doi: 10.1109/TIE.2010.2045998.
[4]   M. I. Mosaad, M. O. El-raouf, M. A. Al-ahmar, and F. M. Bendary, "Optimal PI controller of DVR to enhance the performance of hybrid power system feeding a remote area in Egypt," *Sustainable Cities and Society*, vol. 47, May 2019, doi: 10.1016/j.scs.2019.101469.
[5]   M. F. Roslan, A. Q. Al-Shetwi, M. A. Hannan, P. J. Ker, and A. W. M. Zuhdi, "Particle swarm optimization algorithm-based PI inverter controller for a grid-connected PV system," *PLoS ONE*, vol. 15, no. 12, Dec. 2020, doi:10.1371/journal. pone.024358.
[6]   S. Fahad, A. J. Mahdi, W. H. Tang, K. Huang, and Y. Liu, "Particle swarm optimization based DC-link voltage control for two stage grid connected PV inverter," in *2018 International Conference on Power System Technology (POWERCON)*, 2018, pp. 2233-2241, doi: 10.1109/POWERCON.2018.8602128.
[7]   A. J. Mahdi, S. Fahad, and W. Tang, "An adaptive current limiting controller for a wireless power transmission system energized by a PV generator," *Electronics*, vol. 9, no. 10, Oct. 2020, doi: 10.3390/electronics9101648.

[8]   E. A. Hameed, "Study of grid-connected photovoltaic system," M.Sc. Thesis, Department of Electrical Engineering, Mustansiriayah University, Baghdad, 2019.

[9]   A. Y. Mohammed, "Modeling and simulation of 1MW grid connected photovoltaic system," M.Sc. Thesis, Department of Electrical Engineering, University of Technology, Baghdad, 2017.

[10]   K. Shi, H. Ye, W. Song, and G. Zhou, "Virtual inertia control strategy in microgrid based on virtual synchronous generator technology," *IEEE Access*, vol. 6, pp. 27949–27957, 2018, doi: 10.1109/ACCESS.2018.2839737.

[11]   S. Abdulaziz, G. Attlam, G. Zeki, and E. Nabil, "Cucckoo search algorthim and particle swarm optimization based maximum power point tracking techniques," *Indonesian Journal of Electrical Engineering and Computer Science*, vol. 26, no. 2, pp. 605-616 May 2022, doi: 10.1109/TEC.2012.2219533.

[12]   S. Lavety, R. K. Keshri, and M. A. Chaudhari, "Evaluation of charging strategies for valve regulated lead-acid battery," *IEEE Access*, vol. 8, pp. 164747–164761, 2020, doi: 10.1109/ACCESS.2020.3022235.

[13]   W. S. Abdullah, M. Osman, M. Z. A. Kadir, and R. Verayiah, "Battery energy storage system (BESS) design for peak demand reduction, energy arbitrage and grid ancillary services," *International Journal of Power Electronics and Drive System (IJPEDS)*, vol. 11, no. 1, pp. 398-408, Mar. 2020, doi: 10.11591/ijpeds.v11.i1.pp398-408.

[14]   X. Gao, M. Wang, E. Yue, and W. Muljadi, "Probabilistic approach for power capacity specification of wind energy storage systems eduard muljadi," *IEEE Trans. Ind. Appl.*, vol. 50, no. 2, pp. 1215–1224, 2013, doi: 10.1109/TIA.2013.2272753.

[15]   C. R. Baier *et al.*, "Bidirectional power flow control of a single-phase current-source grid-tie battery energy storage system," in *2015 IEEE 24th International Symposium on Industrial Electronics (ISIE)*, 2015, pp. 1372-1377, doi: 10.1109/ISIE.2015.7281673.

[16]   S. Jadhav, N. Devdas, S. Nisar, and V. Bajpai, "Bidirectional DC-DC converter in solar PV system for battery charging application," in *2018 International Conference on Smart City and Emerging Technology (ICSCET)*, Jan. 2018, doi: 10.1109/ICSCET.2018.8537391.

[17]   A. Chub, D. Vinnikov, R. Kosenko, E. Liivik, and I. Galkin, "Bidirectional DC-DC converter for modular residential battery energy storage systems," *IEEE Transactions on Industrial Electronics*, vol. 67, no. 3, pp. 1944–1955, 2020, doi: 10.1109/TIE.2019.2902828.

[18]   E. Jarmouni, A. Mouhsen, and Z. Benizza, "Energy management in connected and disconnected mode of a photovoltaic system with a battery storage using an artificial neural network technique," *Indonesian Journal of Electrical Engineering and Computer Science*, vol. 23, no. 1, Jul. 2021, pp. 54-62, doi: 10.11591/ijeecs.v23.i1.

[19]   K. Shi, G. Zhou, P. Xu, H. Ye, and F. Tan, "The integrated switching control strategy for grid-connected and islanding operation of micro-grid inverters based on a virtual synchronous generator," *Energies*, vol. 11, no. 6, 2018, doi: 10.3390/en11061544.

[20]   W. Haifeng, "A boost converter design with low output ripple based on harmonics feedback," 2019, *arXiv:1901.10020*.

[21]   S. Fahad, A. Goudarzi, and J. Xiang, "Demand management of active distribution network using coordination of virtual synchronous generators," *IEEE Transactions on Sustainable Energy*, vol. 12, no. 1, pp. 250-261, Jan. 2021, doi: 10.1109/TSTE.2020.2990917.

[22]   U. Bose, S. K. Chattopadhyay, C. Chakraborty, and B. Pal, "A novel method of frequency regulation in microgrid," *IEEE Transaction on Industry Application*, vol. 55, no. 1, pp. 111–121, 2019, doi: 10.1109/TSTE.2020.2990917.

[23]   L. Yang *et al.*, "The strategy of active grid frequency support for virtual synchronous generator," *Electronics,* vol. 10, no. 10, 2021, doi: 10.3390/electronics10101131.

[24]   L. Y. Chuang, H. C. Huang, M. C. Lin, and C. H. Yang, "Particle swarm optimization with reinforcement learning for the prediction of CpG islands in the human genome," *PLoS One*, vol. 6, no. 6, 2011, doi: 10.1371/journal.pone.0021036.

[25]   P. Nammalvar and S. Ramkumar, "Parameter improved particle swarm optimization based direct-current vector control strategy for solar PV system," *Advances in Electrical and Computer Engineering*, vol. 18, no. 1, pp. 105–112, 2018, doi: 10.4316/AECE.2018.01013.

[26]   H. Ghazvinian *et al.*, "Integrated support vector regression and an improved particle swarm optimization-based model for solar radiation prediction," *PLoS One*, vol. 14, no. 5, 2019, doi: 10. 1371/journal.pone.0217634.

[27]   A. A. Esmin, R. A. Coelho, and S. Matwin, "A review on particle swarm optimization algorithm and its variants to clustering high-dimensional data," *Artificial Intelligence Review,* vol. 44, no. 1, pp. 23–45, 2015, doi: 10.1007/s10462-013-9400-4.

[28]   M. V. Kumar and U. Salma, "A novel voltage regulation technique for a three phase grid connected photovoltaic system using fuzzy fractional order pi controller," *International Journal of Recent Technology and Engineering (IJRTE)*, vol. 11, no. 8, pp. 2979–2991, 2019, doi: 10.35940/ijrte.D8937.118419.

[29]   Y. Valle, G. K. Venayagamoorthy, S. Mohagheghi, J. -C. Hernandez, and R. G. Harley, "Particle swarm optimization: basic concepts, variants and applications in power systems," *IEEE Transactions on Evolutionary Computation*, vol. 12, no. 2, pp. 171–195, 2008, doi: 10.1109/TEVC.2007.896686.

[30]   J. H. Thorp and D. C. Rogers, "Thorp and Covich's freshwater invertebrates: ecology and general biology," in *Elsevier,* Amsterdam, vol. 1, 2014. [Online]. Available: https://www.sciencedirect.com/book/9780123850263/thorp-and-covichs-freshwater-invertebrates

[31]   M. Wikelski *et al.*, "Simple rules guide dragonfly migration," *Biology letters,* vol. 2, no. 3, pp. 325–329, 2006, doi: 10.1098/rsbl.2006.0487.

[32]   S. Mirjalili, "Dragonfly algorithm: a new meta-heuristic optimization technique for solving single-objective, discrete, and multi-objective problems," *Neural computing and applications,* vol. 27, no. 4, pp. 1053–1073, 2016, doi: 10.1007/s00521-015-1920-1.

[33]   R. W. Russell, M. L. May, K. L. Soltesz, and J. W. Fitzpatrick, "Massive swarm migrations of dragonflies (Odonata) in eastern North America," *The American Midland Naturalist,* vol. 140, no. 2, pp. 325–342, 1998, doi: 10.1674/0003-0031(1998)140[0325:MSMODO]2.0.CO;2.

[34]   P. R. Hof, and E. V. D. Gucht, "Structure of the cerebral cortex of the humpback whale, Megaptera novaeangliae (Cetacea, Mysticeti, Balaenopteridae," *The Anatomical Record,* vol. 290, no. 1, pp. 1–31. 2007, doi: 10.1002/ar.20407.

[35]   W. A. Watkins and W. E. Schevill, "Aerial observation of feeding behavior in four baleen whales: Eubalaena glacialis, Balaenoptera borealis, Megaptera novaeangliae, and Balaenoptera physalus," *Journal of Mammalogy*, vol. 60, no. 1, pp. 155–63, 1979, doi: 10.2307/1379766.

[36]   J. A. Goldbogen *et al.*, "Integrative approaches to the study of baleen whale diving behavior, feeding performance, and foraging ecology," *BioScience*, vol. 63, no. 2, pp. 90– 100, 2013, doi: 10.1525/bio.2013.63.2.5.

[37]   IEEE Standards Coordinating Committee 21 on Fuel Cells Photovoltaics Dispersed Generation and Energy Storage, *IEEE Recommended Practice for Utility Interface of Photovoltaic (PV) Systems*, vol. 2000. 2000.

BIOGRAPHIES OF AUTHORS

Diana Sabah Obaid ⓘ 🎓 SC Ⓟ is an M.Sc. degree student in the research level at Electrical Engineering Department, University of Technology, Baghdad, Iraq, and complete a B.Sc. degree in 2005 in the Electrical Engineering Department, University of Baghdad, Baghdad, Iraq. Mrs. Diana is interested in Renewable Energy, PV Systems, Storage Energy Systems, and power management. She can be contacted at email: eee.19.38@grad.uotechnology.edu.iq.

Dr. Ali Jafer Mahdi ⓘ 🎓 SC Ⓟ is Assistant Professor in Electrical Engineering. He received B.Sc. and M.Sc. degrees in Electrical Power and Machines from University of Technology (Iraq) in 1995 and 1997, respectively. He received Ph.D. degree from the University of Liverpool (UK) in 2011. He is currently the director of the postgraduate studies at University of Kerbala in Iraq. Also, he is currently the director of Kerbala Journal for Engineering Sciences (KJES) and a scientific member of the Renewable Energy and Power Quality Journal (RE&PQJ). He has served as the Head of Department of Electrical and Electronic Engineering at University of Kerbala (2013-2016). Dr. Ali Jafer Mahdi is also a visiting Lecturer at the South China University of Technology (SCUT) in 2018 and 2019, respectively. He has supervised eight M.Sc. theses, in the field of Control of Renewable Energy Resources and Biomedical Engineering. His research interests include Optimization and Control of Renewable Energy Systems, Power Electronics and Drives, Control of Electrosurgical Generators and Wireless Power Transfer Systems. He has published one book and 36+ scientific papers in peer-reviewed international journals and has more than 313 citations of his work (h-index of 10). He has received four national and international awards and one scholarship. His affiliation is: Department of Electrical and Electronic Engineering, University of Kerbala, Karbala 56001, Iraq. He can be contacted at email: ali.j.mahdi@uokerbala.edu.iq.

Dr. Mohammed Husham Alkhafaji ⓘ 🎓 SC Ⓟ is a lecturer in Electrical Engineering Department. He received B.Sc. and M.Sc. degrees in Electrical Engineering from University of Technology - Iraq in 2004 and 2006, respectively. He received Ph.D. degree from the Cranfield University (UK) in 2017. He has supervised three M.Sc. theses, in the field of Microgrid Control system. His research interests including Optimization and Control of Microgrid system, Electric Vehicles, Renewable Energy Systems, and Power Electronics and Drives. He has published 12+ scientific papers in peer-reviewed international conferences and journals and. His affiliation is: Department of Electrical Engineering, University of Technology, Baghdad, Iraq. He can be contacted at email: m.h.alkhafaji@uotechnology.edu.iq.